

## Supporting Information

### Construction of a Self-Supported Dendrite-free Zinc Anode for High- Performance Zinc-Air Batteries

Chuanheng Mou,<sup>†,‡</sup> Yujia Bai,<sup>‡</sup> Chang Zhao,<sup>‡</sup> Genxiang Wang,<sup>‡</sup> Yi Ren,<sup>†,‡</sup> Yijian Liu,<sup>‡</sup> Xuantao Wu,<sup>‡</sup>  
Hui Wang,<sup>\*,§,‡</sup> Yuhan Sun<sup>\*,†,§,‡</sup>

<sup>†</sup>School of Physical Science and Technology, ShanghaiTech University, Shanghai, 201210, China

<sup>§</sup>Institute of Carbon Neutrality, ShanghaiTech University, Shanghai, 201210, China

<sup>‡</sup>Shanghai institute of cleantech innovation, Shanghai, 201616, China

\*Corresponding author:

Yuhan Sun. e-mail: [sunyh@sari.ac.cn](mailto:sunyh@sari.ac.cn)

Hui Wang. e-mail: [wanghh@sari.ac.cn](mailto:wanghh@sari.ac.cn)

---

## Experimental

1.1 Materials. All chemical reagents are analytically pure. The materials used for the preparation of ZnO nanoparticles are NaOH ( $\geq 98\%$ , Aladdin),  $\text{Zn}(\text{NO}_3)_2 \cdot 6\text{H}_2\text{O}$  (AR, 99%, Aladdin), and zinc foil ( $2 \times 7 \text{ cm}^2$ , 0.3 mm thick, Taobao). Dimethylimidazole (RG, 98%, Tansoole) was used for the synthesis of ZIF-8.

1.2 Preparation of Zn-ZnO@C-X composite electrode. Figure 1a shows the preparation process of the electrode. Before synthesis, the zinc foil was polished with 800C sandpaper, then it underwent ultrasonic cleaning in absolute ethanol for 20 min and ultrapure water for 30 min in sequence for electrode preparation. Firstly, the uniform nano ZnO arrays in situ grown on the zinc foil surface was prepared by adding the pre-processed zinc foil in 100 mL mixed solution of  $\text{Zn}(\text{NO}_3)_2 \cdot 6\text{H}_2\text{O}$  (0.15 g) and NaOH (1.2 g) which was heated to  $70^\circ\text{C}$  2 h<sup>1</sup>. Then ZIF-8 was further grown on the surface of the prepared ZnO arrays (Zn-ZnO@ZIF-8) by placing nano ZnO arrays coated zinc foil in a Teflon-lined reactor containing, 0.15% 2-methylimidazole solution and then being heated to  $70^\circ\text{C}$  for 24 h<sup>2</sup>. After cooling to room temperature, the Zn-ZnO@ZIF-8 composite was obtained and cleaned repeatedly with absolute ethanol and ultrapure water successively, and then dried naturally in air. Lastly, the Zn-ZnO@ZIF-8 composite was converted to Zn-ZnO@C-X (500, 550, 600  $^\circ\text{C}$ ) composite electrodes by annealing Zn-ZnO@ZIF-8 at  $500^\circ\text{C}$ ,  $550^\circ\text{C}$  and  $550^\circ\text{C}$  for 0.5 h in a tubular furnace under Ar atmosphere.

1.3 Preparation of air electrodes. A bifunctional catalyst (Fe-Ni ANC@NSCA)<sup>3</sup> for oxygen reduction reaction (ORR) and the oxygen evolution reaction (OER) was prepared. The bifunctional catalyst slurry was formulated by dispersing Fe-Ni ANC@NSCA and carbon black in propan-2-ol. The bifunctional electrode was fabricated as the following steps: the ink was firstly prepared by dispersing the bifunctional catalyst into a mixture of isopropanol and PTFE; then the prepared ink was sprayed onto the carbon paper (Hesen carbon paper); Finally, the air electrodes were cut into suitable size for assembling the zinc-air full batteries.

1.4 Assembling the Zinc Air Battery. The electrochemical performance of zinc-air battery was investigated on a static cell which is composed of cell body, tetrafluoro gasket, air electrode, stainless steel stop ring, gas diffusion device, cover and zinc related foil. Put the carbon paper coated with bifunctional catalyst into the electrode tank, gas diffusion device with a pin electrode as cathode current collector and zinc foil as anode current collector. The alkaline electrolyte (4M KOH) was injected into the cell body.

1.5 Material Characterization. The morphology and structure of the synthesized materials were characterized using scanning electron microscopy (SEM) with energy-dispersive X-ray spectroscopy (EDS) mapping. The phase and the crystal structure of the samples was analyzed by X-ray diffraction (XRD, Siemens D5000). Diffraction patterns were acquired with Cu-K $\alpha$  radiation between scattering angles of  $3^\circ$ - $50^\circ$  with a scanning rate of  $10^\circ \text{ min}^{-1}$ .

1.6 Electrochemical Characterization. Plating/stripping behaviors of zinc on the bare zinc foil and the Zn-ZnO@C-550 were investigated in a full cell, where air electrode was used as a working electrode and bare zinc foil or the Zn-ZnO@C-550 as both counter and reference electrodes. Galvanostatic plating/stripping test of the full cells was carried out on the electrochemical workstation (PMCCHS08A). Linear polarization curves and anode polarization curves of three-electrode battery with bare zinc foil/Zn-ZnO@C-550 as working electrode, Pt foil as counter electrode and Ag/AgCl electrode as reference electrode were conducted on PAR electrochemical workstation with a scanning rate of  $0.17 \text{ mV s}^{-1}$ ,  $5 \text{ mV s}^{-1}$ , respectively. Galvanostatic discharge/charge measurements of full batteries were performed on a LAND battery-testing instrument. The electrochemical impedance spectra (EIS) in a frequency range from 100 kHz to 0.1 Hz (amplitude: 10 mV). EIS plots at different temperatures were tested (from 30 to  $70^\circ\text{C}$ ). The cyclic voltammetry (CV) at scan rate of 20, 22, 24, 26, 28, 30  $\text{mV s}^{-1}$  were both conducted on PAR electrochemical workstation.

The conductivity is calculated as<sup>4</sup>

$$\sigma = L / (R_{\Omega} \cdot S) \text{ (Eq. 1)}$$

L: Measurement of the effective electrode plate area.

S: Distance between the two pole plates.

1.7 Electric Current distribution. Ansys Fluent can model problems involving the electric potential field by solving the electric potential equation, which can be solved in both fluid and solid zones. The electric potential solver is automatically used with the built-in electrochemical reaction model allowing for the simulation of chemical and electrochemical reactions. The electric potential solver is also used in the Zinc-ion Battery model. When the electric potential solver is enabled, Ansys Fluent solves the following electric potential equation 1 (Eq. 1):

$$\nabla \cdot (\sigma \nabla \phi) + S = 0 \text{ (Eq. 2)}$$

where  $\phi$  is the electric potential,  $\sigma$  is the electric conductivity in a solid zone or ionic conductivity in a fluid zone, and S is the source term.

---

## Results and discussion

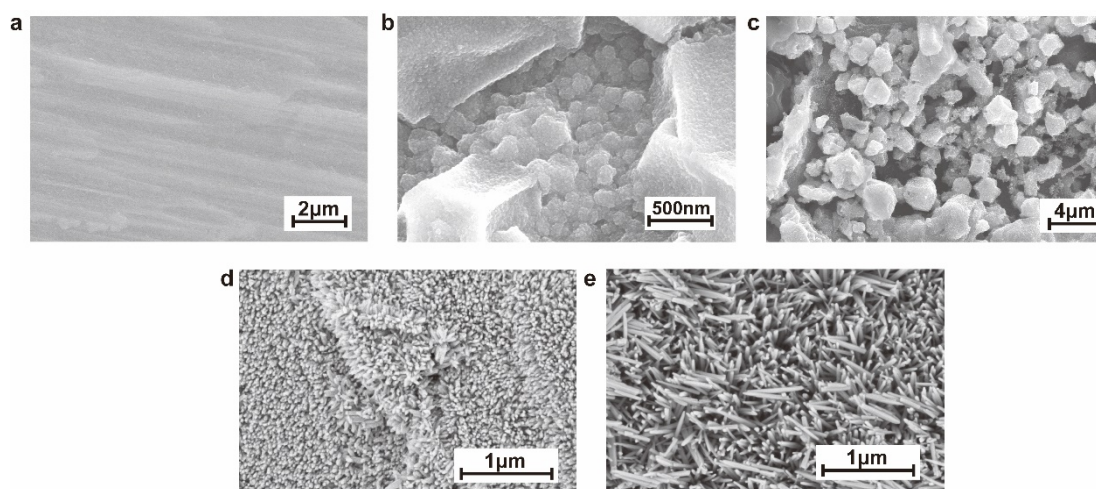


**Figure S1.** SEM images of (a) zinc foil, Zn-ZnO@C-500 (b) and Zn-ZnO@C-600 (c). (d-e) The ZnO nanoarrays prepared at the masses of 0.8 g and 1.6 g of NaOH are shown, respectively.

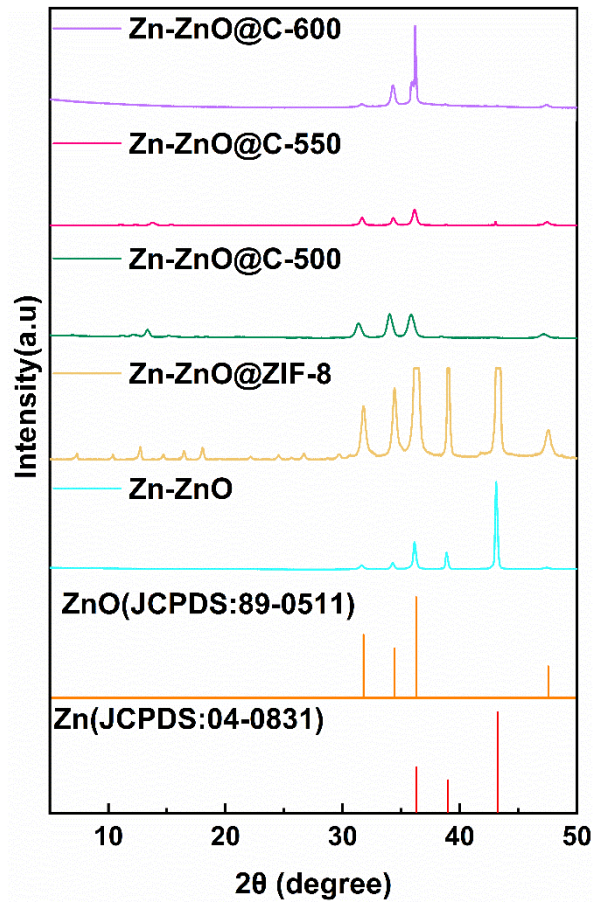


**Figure S2.** XRD pattern of bare zinc foil, Zn-ZnO@ZIF-8 and Zn-ZnO@C-X(500, 550,600 °C) composite electrode.

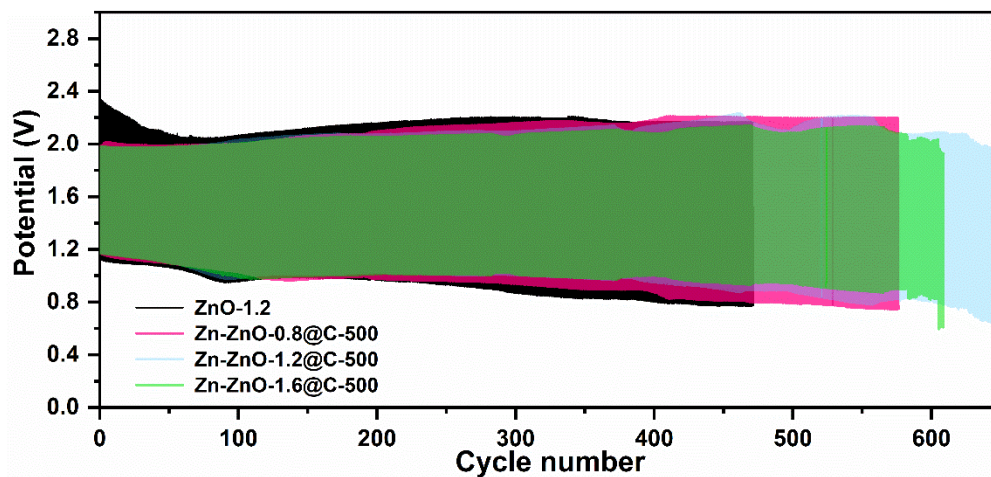


**Figure S3.** The CV curves of Zn-ZnO-X(0.8, 1.2, 1.6)@C-500 cells for NaOH masses of 0.8 g, 1.2 g, and 1.6 g, respectively. The black curve refers to the graph of the full cell life of ZnO prepared at a mass of 1.2 g of NaOH.

**Table S1** Mass fraction of ZnO nanoarray layer.

	W/%
Zn-ZnO-0.8	0.011 %
Zn-ZnO-1.2	0.089 %
Zn-ZnO-1.6	0.097 %

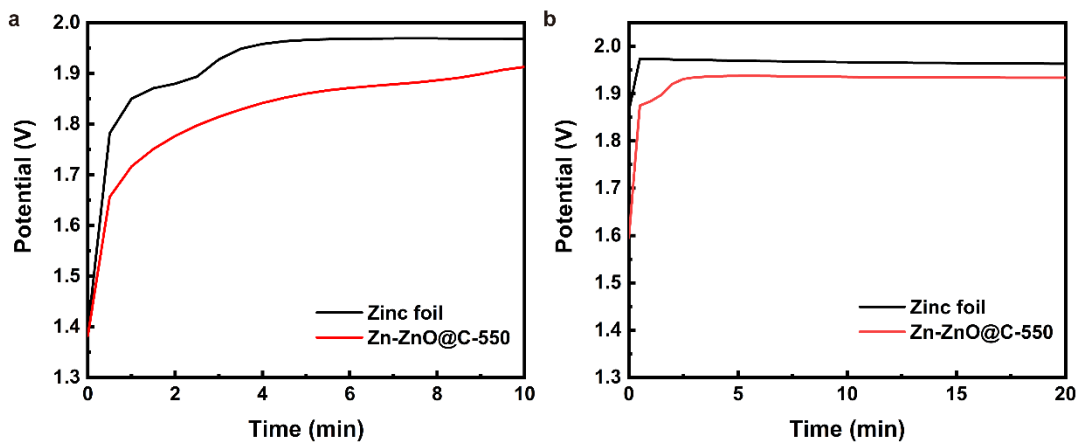
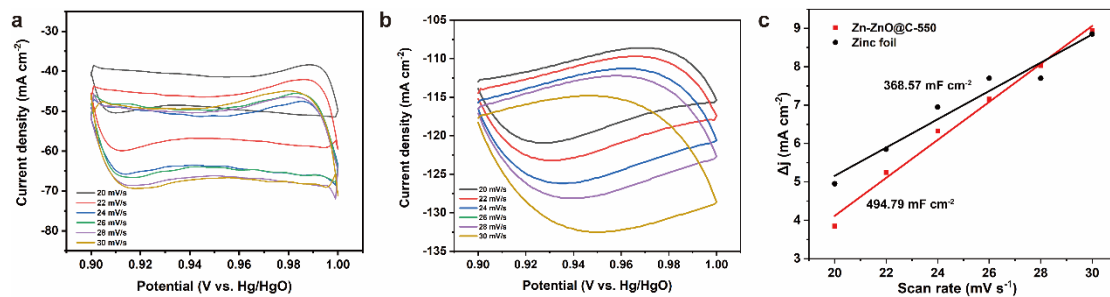


Figure S4. Zn deposition curves at 5 mA cm<sup>-2</sup> on zinc foil and Zn-ZnO@C-550 anodes.



**Figure S5.** (a-b) are the ECSA test plots of Zn-ZnO@C-550 and zinc foil at different sweep speeds, respectively. (c) Plot of the relationship between current density difference and sweep speed.

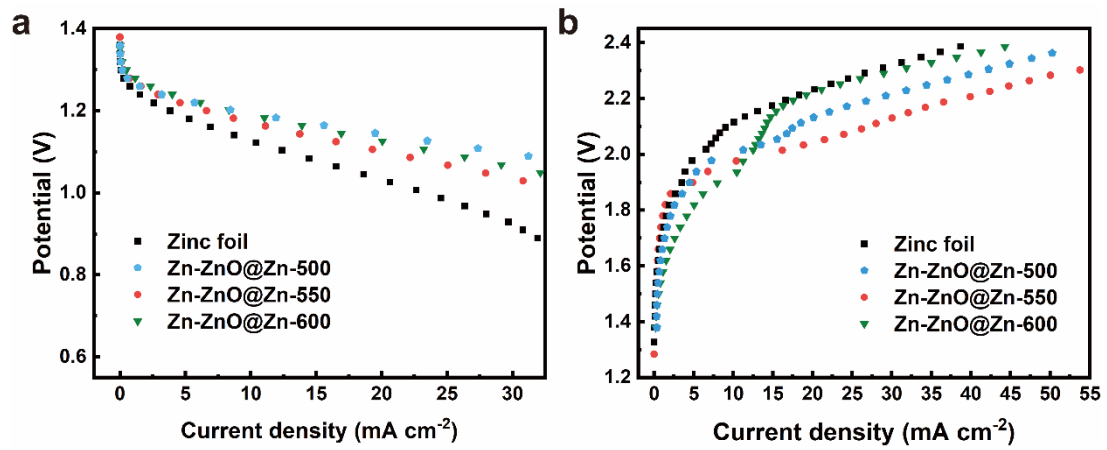


Figure S6. Discharge-charge performance of battery with different anodes.



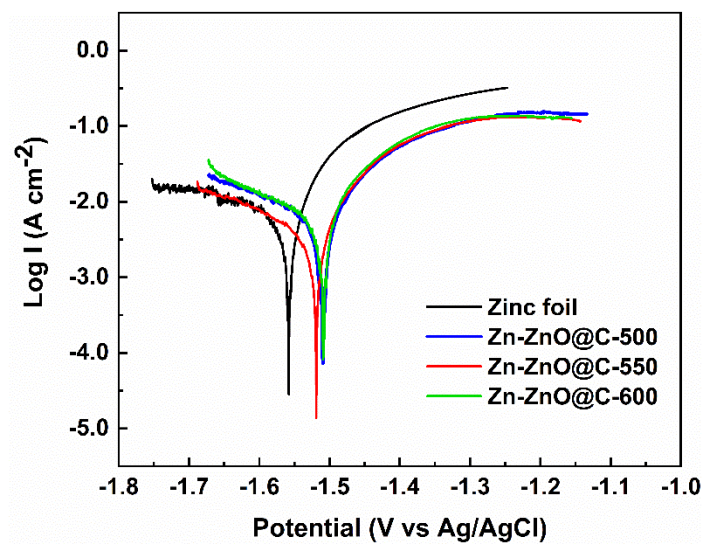
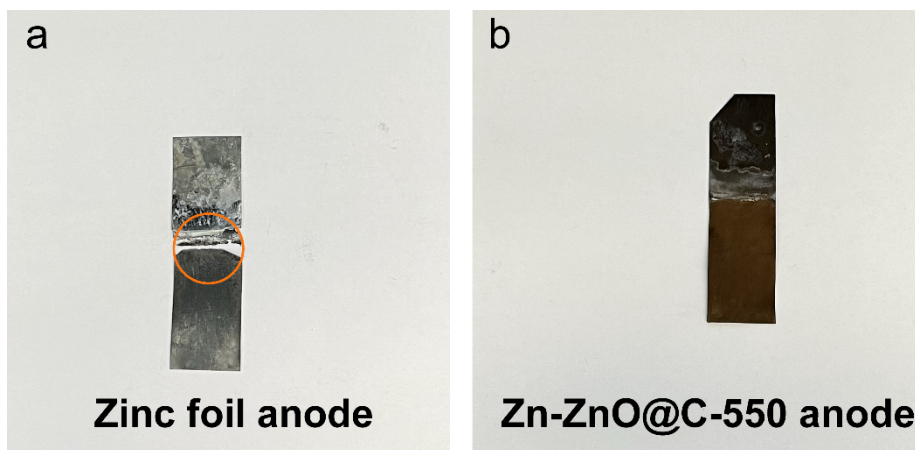


Figure S7. Corrosion resistant performance of battery with different anodes.



**Figure S8.** The zinc foil anode and Zn-ZnO@C-550 anode were immersed in 4M KOH electrolyte for 150 h.

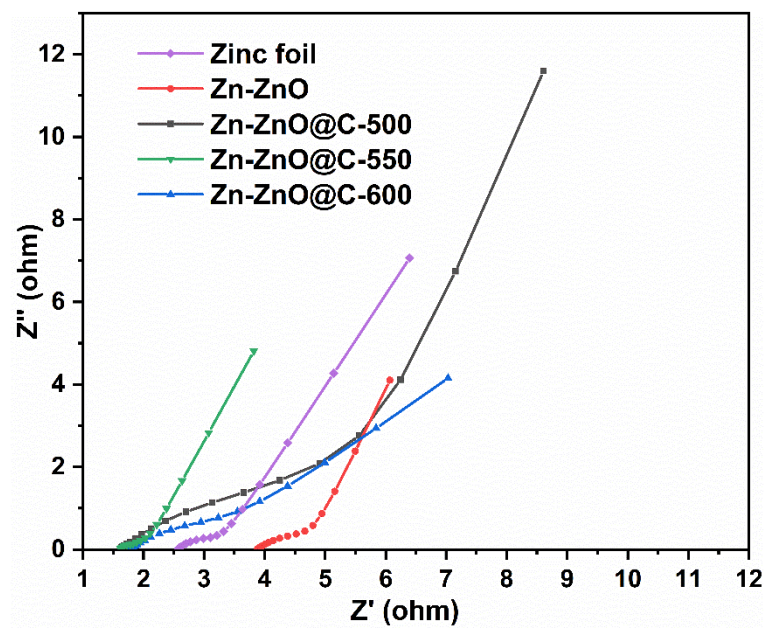


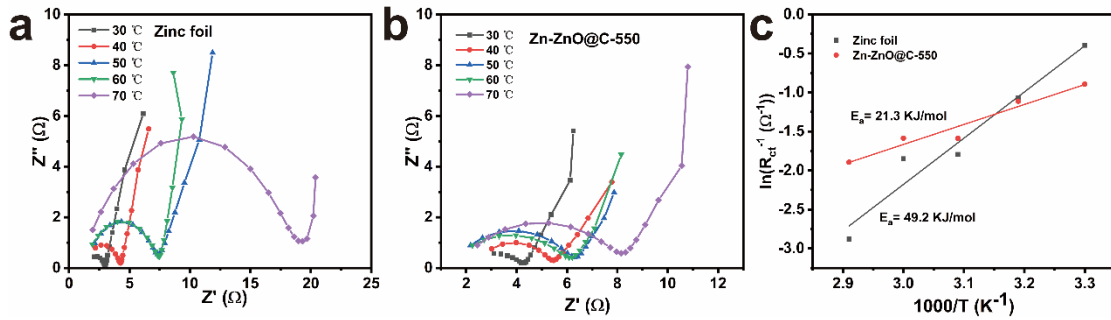
Figure S9. Zn-ZnO@C-X (500, 550, 600), Zn-ZnO and zinc foil impedance tests.

**Table S2.** Impedance data and electrical conductivity of different samples.

Samples	$R_{ct}/\Omega$	$R_s/\Omega$	$\sigma/(\text{ms cm}^{-1})$
Zinc foil	0.8400	2.536	401.7
Zn-ZnO	0.35221	3.863	263.7
Zn-ZnO@C-500	0.7506	1.564	651.3
Zn-ZnO@C-550	0.05490	1.591	640.3
Zn-ZnO@C-600	0.6389	2.328	437.6

**Table S3.** Discharge capacity data of different samples.

Samples	Time/h	Capacity/mAh
Zinc foil	21.93	387.63
Zn-ZnO@C-500	29.91	528.77
Zn-ZnO@C-550	56.32	995.77
Zn-ZnO@C-600	39	689.57

**Figure S10** Nyquist plots of zinc foil and Zn-ZnO@C-550 zinc-air batteries recorded at different temperatures (from 30 °C to 70 °C). Arrhenius plots of inverse  $R_{ct}$  ( $R_{ct}^{-1}$ ) values at different temperatures (from 40 °C to 70 °C).

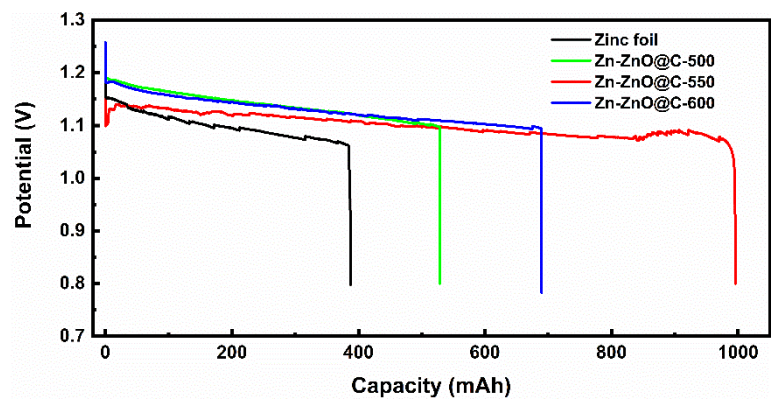


**Figure S11.** The limit discharge curves of battery with different anodes at a current density of 10 mA cm<sup>-2</sup>.

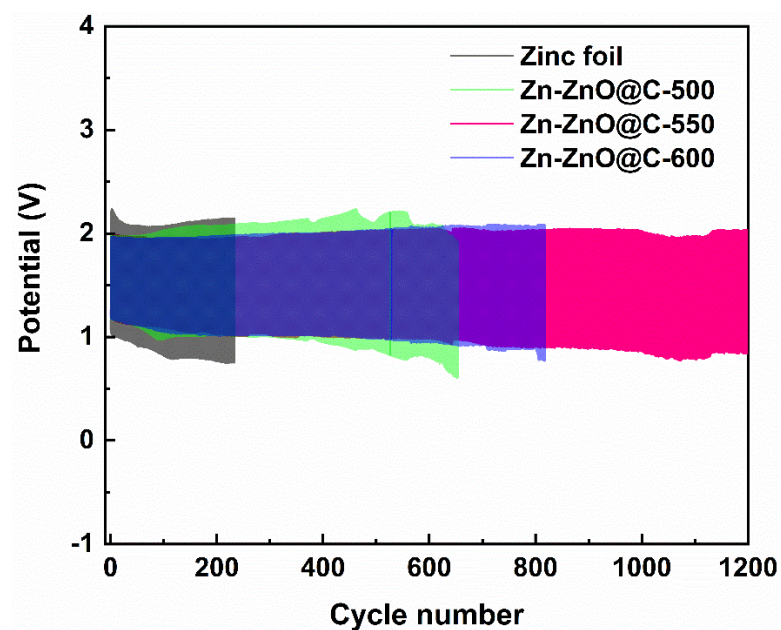


Figure S12. Zn-ZnO@C-X(500, 550, 600), pristine zinc foil electrode cycle life performance test.

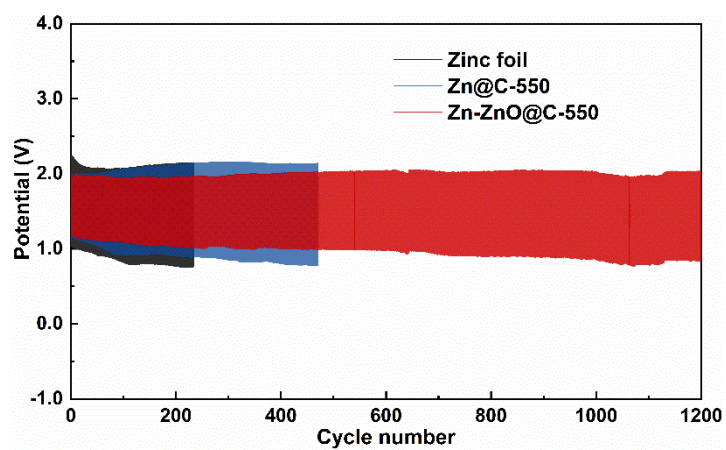
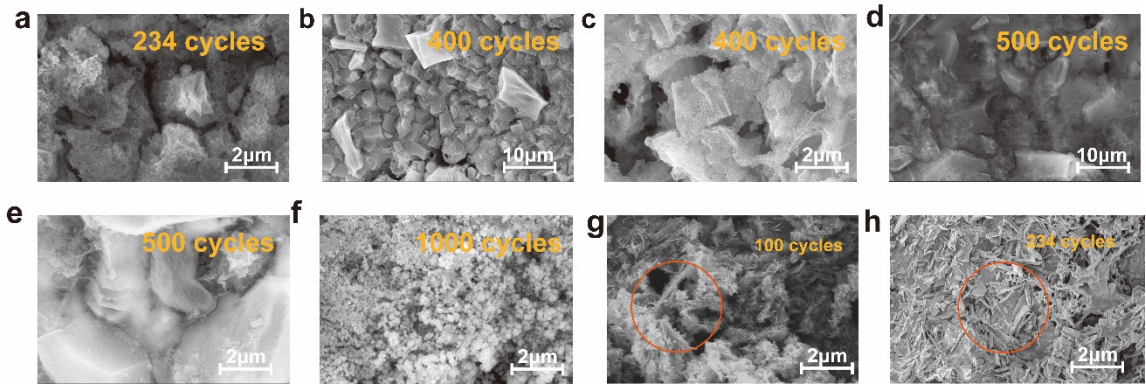


Figure S13 Comparison of the cycle life of Zn foil, Zn@C-550 and Zn-ZnO@C-550 full cells at a current density of  $10 \text{ mA cm}^{-2}$ . (Zn@C-550: Zn@C-550 is a ZIF-8 derived carbon electrode prepared from ZnO using ammonium persulphate<sup>5</sup> as the oxidant.)



**Figure S14.** a-f) SEM of the in Zinc-air battery with Zn-ZnO@C-550 as anode after 234, 400, 500 and 1000 cycles.  
g-h) SEM of the anode in Zinc-air battery with zinc foil as anode.

---

## References

- 1 L.-A. Ma, L.-Q. Hu, T.-L. Guo, Density-Tunable ZnO Nanorod Array Directly Grown on Self-Source Substrate and Field Emission, *液晶與顯示*, 2008, **23**, 357-360.
- 2 W.-w. Zhan, Q. Kuang, J.-z. Zhou, X.-j. Kong, Z.-x. Xie, L.-s. Zheng, Semiconductor@ metal-organic framework core-shell heterostructures: a case of ZnO@ ZIF-8 nanorods with selective photoelectrochemical response, *Journal of the American Chemical Society*, 2013, **135**, 1926-1933.
- 3 H. Li, X. Shu, P. Tong, J. Zhang, P. An, Z. Lv, H. Tian, J. Zhang, H. Xia, Fe-Ni Alloy Nanoclusters Anchored on Carbon Aerogels as High-Efficiency Oxygen Electrocatalysts in Rechargeable Zn-Air Batteries, *Small*, 2021, **17**, 2102002.
- 4 V. Parameswaran, N. Nallamuthu, P. Devendran, E. Nagarajan, A. Manikandan, Electrical conductivity studies on Ammonium bromide incorporated with Zwitterionic polymer blend electrolyte for battery application, *Physica B: Condensed Matter*, 2017, **515**, 89-98.
- 5 R. Yuksel, O. Buyukcakil, W. K. Seong, R. S. Ruoff, Metal-Organic Framework Integrated Anodes for Aqueous Zinc-Ion Batteries, *Advanced Energy Materials*, 2020, **10**.